



Strathprints Institutional Repository

**Luque, Antonio and Anaya-Lara, Olimpo and Leithead, William (2013)
Control of DFIG wind turbines in offshore networks during large
transients. In: EWEA 2013, Vienna, Austria, 2013-02-04 - 2013-02-07,
Messe Wien Exhibition & Congress Center. ,**

This version is available at <http://strathprints.strath.ac.uk/57573/>

Strathprints is designed to allow users to access the research output of the University of Strathclyde. Unless otherwise explicitly stated on the manuscript, Copyright © and Moral Rights for the papers on this site are retained by the individual authors and/or other copyright owners. Please check the manuscript for details of any other licences that may have been applied. You may not engage in further distribution of the material for any profitmaking activities or any commercial gain. You may freely distribute both the url (<http://strathprints.strath.ac.uk/>) and the content of this paper for research or private study, educational, or not-for-profit purposes without prior permission or charge.

Any correspondence concerning this service should be sent to Strathprints administrator: strathprints@strath.ac.uk

Coordinated control for DFIG wind farms and VSC-HVDC transmission to enhance FRT capability for offshore ac star layout

Antonio Luque⁽¹⁾, Olimpo Anaya-Lara⁽²⁾, William E Leithead⁽³⁾, Grain P. Adam⁽⁴⁾

University of Strathclyde,
Department of Electronic and Electrical Engineering
Royal College Building
204 George Street, Glasgow
G1 1XW

Antonio.Luque@strath.ac.uk⁽¹⁾, olimpo.anaya-lara@strath.ac.uk⁽²⁾, w.leithead@strath.ac.uk⁽³⁾,
grain.adam@strath.ac.uk⁽⁴⁾

Abstract

Control, flexibility and the fault ride-through capability of large offshore wind farms, variable-speed wind turbines and their system array are studied in this paper. The research is focused on the implementation of different control techniques for VSC-HVDC links and their assessment during large transients. Improvements in the VSC control system have been introduced. The third harmonic injection technique and accurate control of the dc voltage for the HVDC links to improve the modulation signal, which is fitted into the PWM system. Improvements in data acquisition and the processing of the reference signals for the inner and outer current controller have shown significant power peaks reduction during large transients. Particular attention is paid to fault current reduction and the improvement in recovery time. The control system has also improved considerably the dc voltage performance in the HVDC links.

Overall, results have shown significant improvements in the active and reactive power transmission for the ac star wind farm layout and the HVDC links.

This focuses in particular upon the control system of the HVDC and WTs, the active and reactive power performances and the fault ride-through capability of the ac star layout. The investigation was conducted in Matlab/Simulink, which provides tools for modeling, simulating and analyzing in multi-domain dynamic systems.

Keywords: Offshore wind power, active and reactive power control, frequency controller, fault ride-through capability, HVDC networks.

I. Introduction

In spite of economic crisis significant numbers of countries are investing in the wind energy sector. Consequently, this engineering sector is growing fast and seems to have a great potential. Due to this, the expanding wind energy sector will have an important role in the control of the electrical network [1],[2].

The increasing energy production for a singular wind turbine and the rapid development of large scale offshore wind farms will produce an important impact contribution to the grid. It is probable that offshore input will soon replace onshore conventional power stations [3].

Although, offshore networks (into deep water) are under development there are not many examples of power control for HVDC links; it seems that the VSC system could be the best solution to control and transfer large quantities of power from offshore power into the grid. The VSC technique has already proven its reliability in transferring power in shallow water [4]. It has also shown high efficiency in terms of mixed power from diverse energy sources (i.e.: wind energy and gas & oil power stations) [3],[5],[6], [7]. It also has a higher flexibility to re-direct power during large transients or periods of fluctuating demand. Therefore, this control system of HVDC has become more attractive than classical HVDC controller [8]. In addition, the VSC control system can exchange power in real time without causing problems in the offshore grid.

The goal of this study is to evaluate the performance of the VSC-HVDC system connected to DFIG WFs during large transients in the ac star offshore layout. This report has also study fault ride-through capability of the VSC control system.

II. Wind Farm Layout

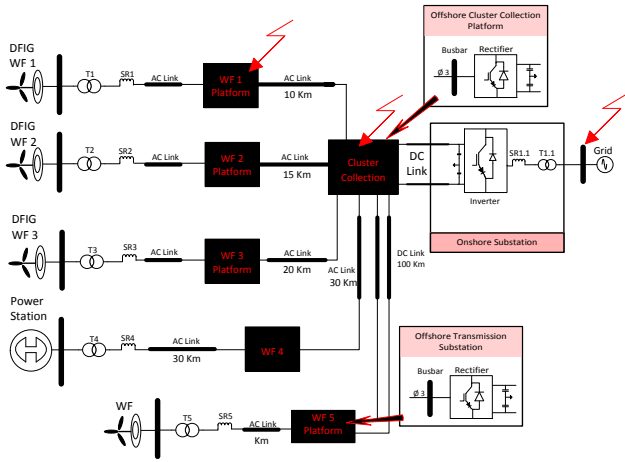


Figure 1: Wind farm layout "single-point connection"

Fig. 1 illustrates the configuration of the ac start layout. DFIG WFs are connected to their own offshore substations where voltage is stepped up from 33 kV to 132 kV and then transferred to the cluster collection platform. Finally, through the point-to-point HVDC system, offshore power is delivered to the onshore substation. Implementations in the control system in the VSC-HVDC link and in the DFIG WT can be written:

VSC-HVDC:

1. The P/f and V_{dc}/f Controllers
2. Accurate control of the dc voltage
3. Third harmonic injection technique

DFIG WT:

1. The P/f Controller
2. Reactive power control "Rotor side converter and/or Grid side converter"
3. I_{dq} signal improvements

III. System Control

The system control is based upon VSC technology. The VSC control system decouples the active and reactive power, frequency, ac/dc voltages and ac current to create appropriated modulation signals used in PWM systems which commutate on/off switches in the back - to - back converters [9].

A. Reference signals

The VSC system transforms electrical network parameters into numerical values which are used to control the HVDC system. Through this transformation it is possible to create specific reference signals for the inner and outer current controller [10, 11]. Depending on the transformation setting the i_{dref} is associated to the active power and

V_{dc} voltage control and the i_{qref} is generally the reference value for the reactive power control. The controlling errors between the expected and the produced power; thus through the inner and outer current controller the active power and the reactive power are adapted to the system requirements. Therefore, powers can be re-directed under abnormal operation.

Both reference signals should be limited to prevent the back- to- back converters from high fault currents during transients [12].

Fig. 2 illustrates transformation of the sinusoidal phases into dq .

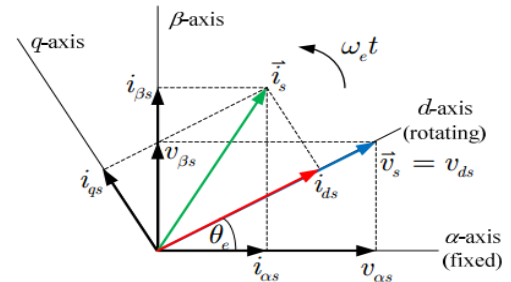


Figure 2: Phasor Diagram

B. VSC-HVDC System: Modeling and Control

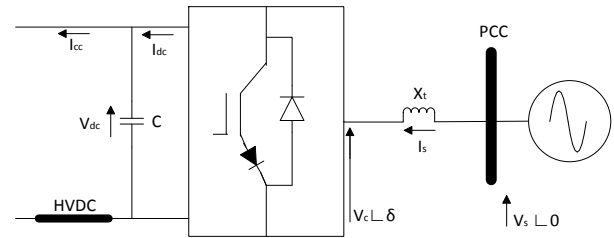


Figure 3: Equivalent circuit of the VSC-HVDC three-phase in dq -frame

VSC features provide greater benefits than traditional LCC systems, i.e. communication between converters is almost instantaneous. The control system can react from abnormal circumstances faster than the LCC [7, 13]. It can also change power flow direction without creating significant hazards in the electrical network, so power can be re-directed (leading or lagging) helping the system to recover from large transients [8]. The VSC system also allows for exchanging power with different networks without altering its ac autonomy, so it becomes more reliable than the LCC [7, 9, 14].

The active and the reactive power in figure 3 are controlled by the difference between the receiving voltage angle in the converter " δ " and the sending voltage angle in the PCC "0" [10, 15]. As was mentioned before, depending on the angle position, converters can send power to the grid or receive

power from the grid. The mathematical model based on the dq reference frame is given [16]:

B1. Control of the dq -Frame

abc reference frame:

$$\frac{di_{sabc}}{dt} = -\frac{R}{L}i_{sabc} + \frac{1}{L}(V_{sabc} - V_{cabc}) \quad (1)$$

dq reference frame:

$$V_{sd} = R * i_{sd} + L \frac{di_d}{dt} - wLi_{sq} + V_{sd} \quad (2)$$

$$V_{sq} = R * i_{sq} + L \frac{di_q}{dt} - wLi_{sd} + V_{sq} \quad (3)$$

Power balance AC/DC:

$$V_{sdc}I_{dc} = \frac{3}{2}(V_{cd} * i_{sd} + V_{cq} * i_{sq}) \pm CV_{dc} \frac{dV_{dc}}{dt} \quad (4)$$

The active and the reactive power can be written [9]:

$$P = \frac{3}{2}[V_d i_d + V_q i_q] = \frac{3}{2} V_d i_d \quad (5)$$

$$Q(t) = \frac{3}{2}[-V_d i_q + V_q i_d] \approx 0 \quad (6)$$

B2. PWM Control System

The VSC system uses a PWM modulation to transform the ac modulation signal obtained through the inner and outer current controller into dc voltage. The ratio of the transformed signal is controlled by the index modulation which is the difference between the maximum ac voltage that the system can generate and the dc voltage in the HVDC link. The index modulation should be equal to or smaller than 1 ($|m| \leq 1$). Otherwise, if index modulation is greater than 1, the system will reach over-modulation and become unstable [9, 10]. Equations 7, 8 and 9 show the relationship between index modulation and ac/dc voltages in the dq -frame. δ is the load angle and m is the index modulation.

$$V_{cd} = \frac{1}{2}MV_{dc} + \cos\delta \quad (7)$$

$$V_{cq} = \frac{1}{2}MV_{dc} + \sin\delta \quad (8)$$

$$m = \frac{2 * \widehat{V}_{ac}}{\widehat{V}_{dc}} \quad (9)$$

B3. Inner and Outer Current Controller

In order to design control loops for the inner and outer current controller, equation (2) is decoupled follow by [6, 17]:

$$V_{sd} = U_d - wLi_q + V_{sq} \quad (10)$$

$$V_{sq} = U_q + wLi_d + V_q$$

Developing V_{sdq} into new signals, U_{dq} becomes:

$$U_d = R * i_{sd} + L \frac{di_{sd}}{dt} = k_{pi}(i_{sd}^* - i_{sd}) + k_{ii} \int (i_{sd}^* - i_{sd}) dt \quad (11)$$

$$U_q = R * i_{sq} + L \frac{di_{sq}}{dt} = k_{pi}(i_{sq}^* - i_{sq}) + k_{ii} \int (i_{sq}^* - i_{sq}) dt$$

k_{pi} and k_{ii} are proportional and integrals gains.

Fig. 4 shows the basic structure of an inner and outer current controller for active power controller.

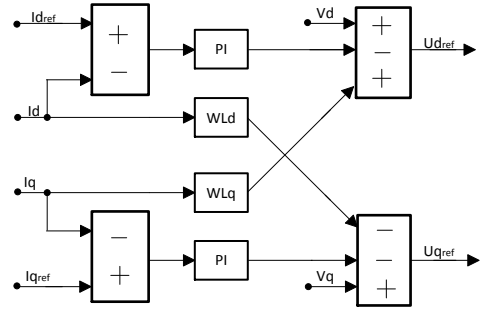


Figure 4: Inner and Outer current controller loop

B4. The P/f Controller

The P/f controller reacts to change in the energy demand and also correspondingly to alteration of the frequency [9, 18-20]. Hence, this controller becomes more efficient during large transients.

Fig. 5 shows schematic control of the P/f controller in VSC scheme.

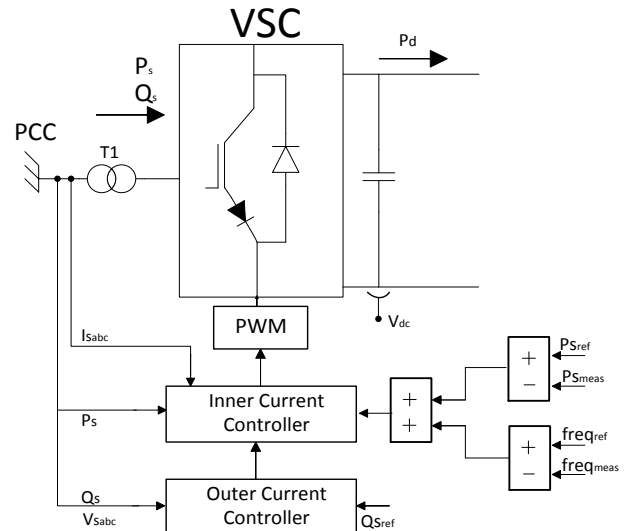


Figure 5: p/f controllers of the VSC system

A mathematical approach can be written:
The frequency of the system can be written as:

$$f - f_o = k(P - P_o) \quad (12)$$

To obtain the frequency reference signal can be controlled by:

$$e_f = k_{pi} \int (f - f_o) dt \quad (13)$$

Then finally the referential signals are introduced in the inner and outer current controller (i_d^*).

$$i_d^* = \int e_f + i_d dt \quad (14)$$

B5. Third harmonic injection

The third harmonic injection is a technique which modifies ac voltage modulation signals. Basically, it reduces the maximum amplitude of modulation signals [21]. This allows increasing ac voltage output by 15% before the over-modulation region is reached. Therefore, the index modulation can be increased 15% and consequently, there is a direct improvement in the active, reactive power and dc power transferred [9].

Figure 6 shows the modulating signal corresponding to the third harmonic injection technique.

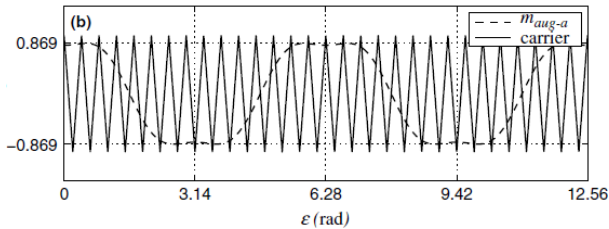


Figure 6 this plot is taken from the book: Voltage-Source Converter in Power System: Modeling Control and Applications [9].

B6. Fault Ride-Through Capability (FRT)

Previously, due to low wind power input into the grid, wind farms were not allowed to remain connected during large transients. Nowadays, or in the near future wind power input will be considerably higher than in the last decade. Hence, wind farms must remain connected to the grid and help to recover ac voltage during large transients [19, 22, 23].

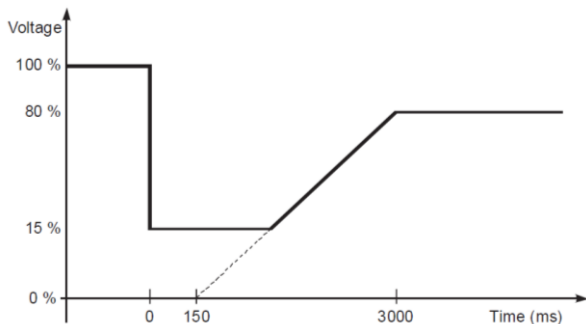


Figure 7 Fault ride-through capability voltage profile.

Requirements of the UK grid for large transients can be given by [19]:

- Wind farms must remain stable during transient's duration. Maximum time to recover ac voltage for the UK grid code is 140 ms.
- Within 0.5s voltage pre-fault value must be restored at 90%.
- Terminal voltage of the offshore wind farms should not be less than 15% during transient periods.
- During the fault period where the voltage is outside the limits specified in CC.6.1.4, the wind farms and dc converters must generate the maximum reactive power possible without exceeding their thermal ratings [19].

IV. Case Studies

The case study is a point-to-point offshore connection for ac star layout (see Figure 1). Figure 1 represents the ac star layout where five wind farms are connected to a cluster collection platform and then through a HVDC link; active and reactive powers are subsequently transferred to an onshore platform. The first four wind farms are connected through their own collection platform to the cluster collection platform by ac cables. The fifth wind farm is linked to the cluster by a dc link. The first three wind farms have DFIG wind turbines which are connected to their own collection platforms and then they are connected to the cluster collection platform by ac cables, 10, 15 and 20 Km in length respectively. The fourth wind farm is a conventional synchronous power station which maintains the system frequency, this power station is linked to the cluster by ac cables in length of 30 Km. Finally, the last wind farm is connected to the cluster collection platform by dc cables of a length of 100 Km.

Total power transfer from offshore to onshore is 550 MVA. Thus, total power transferred is divided into three DFIG wind farms which produce 50 MVA, one gas & oil power station which produces 200 MVA and a separate wind farm which produces 200 MVA. Wind turbines are linked to the collection platform by ac cables rated at 33 kV and then the wind farms are linked to the cluster by ac cables rated at 132 kV. Finally, both HVDC links are rated at ± 150 kV. To analyse the dynamic performance and fault ride-through capability of this ac star layout, three transients have been applied in wind farm 1, the cluster collection platform and in the onshore substation.

V. Simulation Results

In this section the capability of the ac star layout to recover from large transients is investigated. This layout is used to compare the different VSC control techniques for active and reactive power. In order to see the performances of wind farm collection platforms, the cluster collection platform and in the grid, there have been installed different measurement points in which voltage, current and powers are obtained and then processed to obtain values which are used to evaluate the ac start layout and HVDC links performances.

A.1 V-I and P-Q performances at Wind Farms Collection Platform

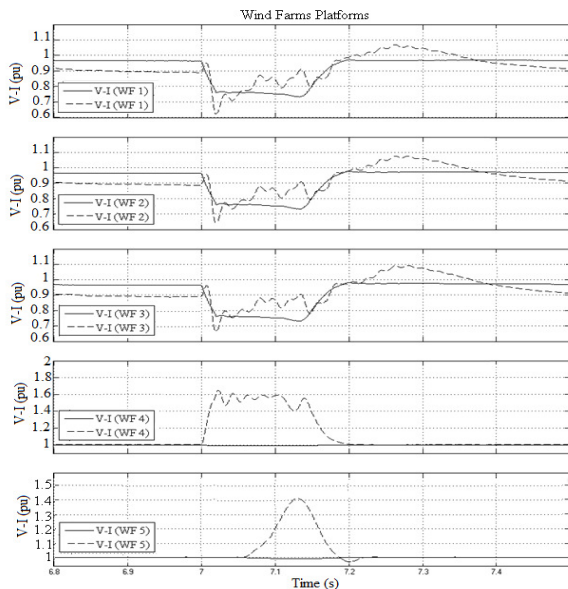


Figure 8 shows voltage and current performances of five wind farms at collection platforms.

Due to the implementation of the mentioned control techniques for the VSC-HVDC system, it has been discovered that these improvements influence the current performance of the ac star layout. As can be seen in Figure 8, the WF 4 shows a significant current decreased during the large transients at 7s. The current drops by almost 0.5 pu. The value of fault current has dropped especially in the beginning and at the end of the transient. This also is clear to see in the power performances in WFs collection platforms (Figure 9). During this transient the reactive power performs just over 300 MVar but with a simple active and reactive power controller; the reactive power is much higher than 300 MVar. The controller also significantly improves the recovery time of the ac star layout.

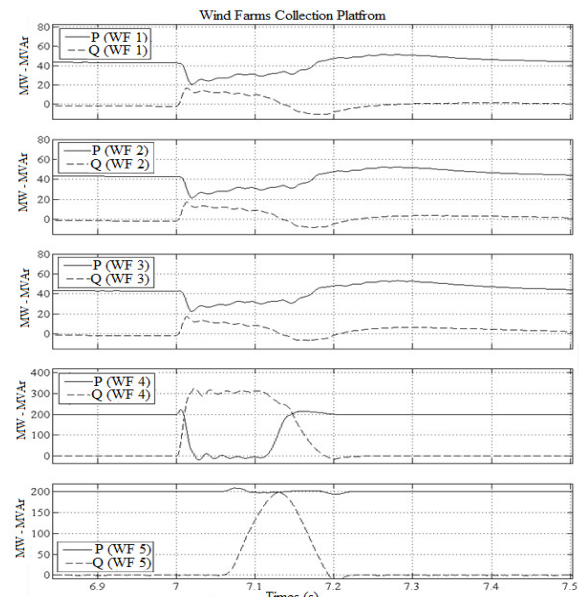


Figure 9 shows active and reactive power performances of five wind farms at collection platforms

A.2 V-I Performances Cluster collection Platform

Figure 10 shows the voltage and current performances of four wind farms connected to the cluster collection.

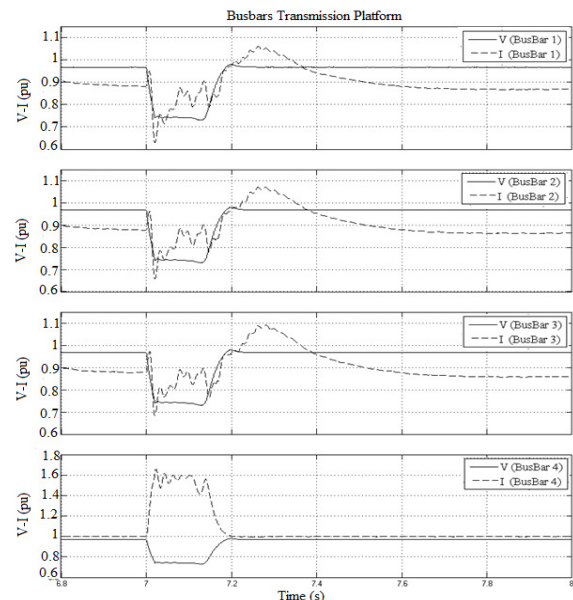


Figure 10 shows performances of the voltage and the current performances.

Figure 10 again shows improvement in the current performance of the WF 4. The current performance is significantly improved at the end of the transient. At the end of the transient, the current peak has been decreased by 0.5 pu. Improvement in the fault current has improved the reactive power performance.

A.3 HVDC Link

This figure is divided into two plots. Plot 1 shows performance of the dc voltage (\pm dc voltage) on the rectifier (cluster collection platform) and the second plot shows also performance of the dc voltage in the inverter side (onshore substation).

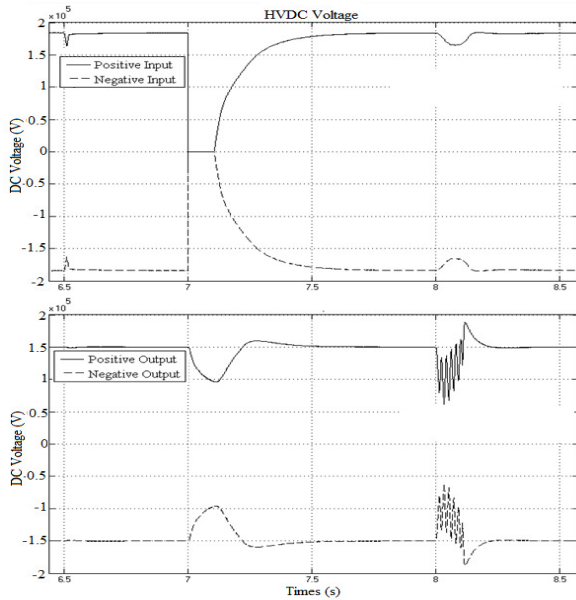


Figure 11 dc voltage in the HVDC link

Introduction of the mentioned controllers in the VSC control system have significantly improved the fault ride-through capability of the HVDC link. These control system improvements also improve peaks of the dc voltage during the transient at 8s. It has become slightly smaller. Unfortunately, troughs of the dc power have become bit higher.

Overall the \pm dc voltage fluctuations have also reduced and the recovery time of the HVDC link is reduced significantly enough that it recovers the steady state almost instantly.

A.4 V-I Performances in the Grid

Figure 12 shows the performance of the voltage and current in the grid with a simple active and reactive power controller.

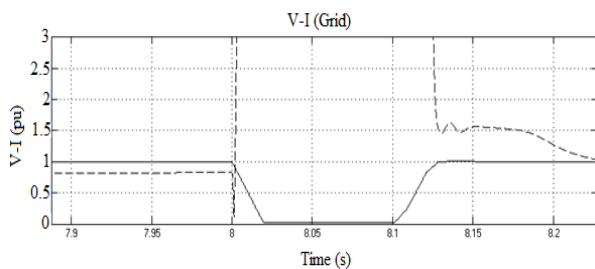


Figure 12 shows performance of V-I in the grid side.

Figure 13 shows the performance of the voltage and current in the grid with P/f, V_{dc}/f , accurate control of the dc voltage and third harmonic injection technique.

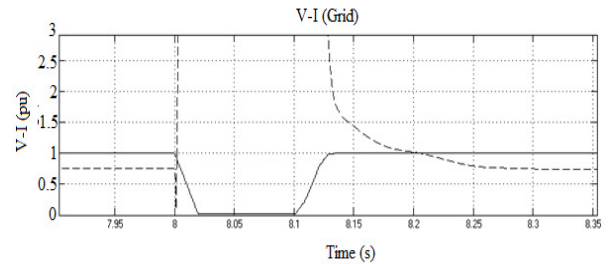


Figure 13 shows performance of V-I in the grid side

Comparing both figures (12 and 13) it is clear to see that improvements in the VSC control system have enhanced current performance. Decreasing current peak and reducing recovery time of the grid current have enhanced performance of the HVDC link too.

V. Conclusions

This paper investigated the viability of using voltage source converter HVDC networks to facilitate the integration of large offshore wind farms into the electrical network.

Based upon the results presented in this paper, it is possible to conclude:

- Implementations of P/f, V_{dc}/f , accurate control of the dc voltage and third harmonic injection technique have enhanced VSC performance, increasing reliability and viability of the HVDC links.
- The active and reactive power performances during large transients have been considerably improved, reducing fluctuations of the ac/dc system: peaks and troughs.
- The VSC control system has also reduced the recovery time of the ac star layout and HVDC links from large transients. Consequently this has improved the fault ride-through capability of this system.
- Results have shown that HVDC links can be connected to the grid during entire transients.
- This ac layout has increased reactive power transmission. Consequently the active power and the power factor of the ac star layout have been reduced.
- This ac star layout forces the installation of ac filters in the cluster collection platform to adequate reactive power transmission, so increasing total price of the installation.
- Controlling the voltage and the current of the VSC-HVDC system from the conventional power station; it has been noticed that it considerably influences the performance of the WF 4.

Unfortunately it does not influence the performance of the other three wind farms connected by ac cables. Therefore, future research should focus on current control in the cluster collection platform.

- These improvements in the VSC control system should facilitate integration of large offshore wind farms into different electrical networks.

References

1. Bilgili, M., A. Yasar, and E. Simsek, Offshore wind power development in Europe and its comparison with onshore counterpart. *Renewable and Sustainable Energy Reviews*, 2011. **15**(2): p. 905-915.
2. Association, E.W.E., *Oceans of opportunity*, 2009, Ewea.
3. Anaya-Lara, O., et al., Rotor flux magnitude and angle control strategy for doubly fed induction generators. *Wind energy*, 2006. **9**(5): p. 479-495.
4. Wu, B., *High-power converters and AC drives* 2006: Wiley-IEEE Press.
5. Ekanayake, J.B., L. Holdsworth, and N. Jenkins, Comparison of 5th order and 3rd order machine models for doubly fed induction generator (DFIG) wind turbines. *Electric Power Systems Research*, 2003. **67**(3): p. 207-215.
6. Feltes, C., et al., Fault Ride-Through of DFIG-based Wind Farms connected to the Grid through VSC-based HVDC Link. *Proc. 16th PSCC*, Glasgow, 2008: p. 7.
7. Friedrich, K. Modern HVDC PLUS application of VSC in modular multilevel converter topology. in *Industrial Electronics (ISIE)*, 2010 IEEE International Symposium on. 2010.
8. Grain Philip Adam, O.A.-L., *Flexible AC Transmission Systems (FACTS) Devices*. University of Strathclyde, Electronic and Electrical Engineering Department Power Electronics, Drives and Energy Conversion Group, 2011: p. 25.
9. Arrillaga, J., Y.H. Liu, and N.R. Watson, *Flexible Power Transmission: The HVDC Options 2007*: Wiley Online Library.
10. Xiaoguang, W. and T. Guangfu. Research of AC/DC Parallel Wind Farm Integration Based On VSC-HVDC. in *Power System Technology*, 2006. PowerCon 2006. International Conference on. 2006. IEEE.
11. Yazdani, A. and R. Iravani, *Voltage-Sourced Converters in Power Systems: Modeling, Control, and Applications 2010*: Wiley Online Library.
12. Liang, J., et al. Control of multi-terminal VSC-HVDC transmission for offshore wind power. 2009. IEEE.
13. Mokryani, G., et al., Improving Fault Ride-Through Capability of Variable Speed Wind Turbines in Distribution Networks.
14. Giddani, K., Control Design and Stability Assessment of VSC-HVDC networks for Large-Scale Offshore Wind Integration, in *Department of Electronic and Electrical Engineering 2012*, University Of Strathclyde: Glasgow. p. 1-238.
15. Machowski, J., J. Bialek, and J. Bumby, *Power system dynamics: stability and control* 2011: Wiley.
16. Giddani, K., *Voltage Source Converter (VSC) and Associated Control*. University of Strathclyde, Institute of Energy and Environment, 2011: p. 25.
17. Giddani O. A, et al., Grid Integration of a Large Offshore Wind farm using VSC-HVDC in parallel with an AC submarine cable.pdf. IEEE, 2010.
18. Gomis-Bellmunt, O., et al. Multiterminal HVDC-VSC for offshore wind power integration. 2011. IEEE.
19. Giddani, O., et al. Control strategies of VSC-HVDC transmission system for wind power integration to meet GB grid code requirements. in *Power Electronics Electrical Drives Automation and Motion (SPEEDAM)*, 2010 International Symposium on. 2010. IEEE.
20. Haileselassie, T.M. and K. Uhlen. Frequency sensitivity analysis of ac grids connected to MTDC grid. in *AC and DC Power Transmission*, 2010. ACDC. 9th IET International Conference on. 2010. IET.
21. Holmes, D.G. and T.A. Lipo, *Pulse Width Modulation for Power Converters: Principles and Practice*, 2003, 2003, IEEE Press.
22. Freris, L. and D. Infield, *Renewable energy in power systems* 2008: Wiley.
23. Mueeen, S., *Wind Energy Conversion Systems: Technology and Trends 2012*: Springer.